

Optical and structural characteristics of Y_2O_3 thin films synthesized from yttrium acetylacetonate

G. Alarcón-Flores · M. Aguilar-Frutis · M. García-Hipólito ·
J. Guzmán-Mendoza · M. A. Canseco · C. Falcony

Received: 28 September 2007 / Accepted: 19 February 2008 / Published online: 23 March 2008
© Springer Science+Business Media, LLC 2008

Abstract Yttrium oxide thin films are deposited on silicon substrates using the ultrasonic spray pyrolysis technique from the thermal decomposition of a β -diketonate, yttrium acetylacetonate ($Y(acac)_3$). The decomposition of $Y(acac)_3$ was studied by thermogravimetry, differential scanning calorimetry, mass spectrometry, and infrared spectroscopy. It was found that a β -diketone ligand is lost during the initial steps of decomposition of the $Y(acac)_3$. The rest of the complex is then dissociated or degraded partially until Y_2O_3 is obtained in the final step with the presence of carbon related residues. Then the $Y(acac)_3$ was used to synthesize Y_2O_3 thin films using the spray pyrolysis technique. The films were deposited on silicon substrates at temperatures in the range of 400–550 °C. The films were characterized by ellipsometry, infrared spectroscopy, atomic force microscopy, and X-ray diffraction. The films presented a low surface roughness with an index of refraction close to 1.8. The crystalline structure of the films depended on the substrate temperature; films deposited at 400 °C were mainly amorphous, but higher deposition temperatures (450–550 °C), resulted in polycrystalline with a cubic crystalline phase.

Introduction

Metallic and rare-earth oxides thin films such as ZrO_2 , HfO_2 , Y_2O_3 , La_2O_3 , Al_2O_3 , etc., have been studied due to their applications in several areas of technological interest. For example, because of their wide energy band gap, some of these oxides are used as host matrix on the fabrication of luminescent materials [1]. Also, they are studied as optical layers [2], as protective or antireflection layers, as well as detectors [3–6]. Thin films of materials such as ZrO_2 , Y_2O_3 , and Al_2O_3 have shown an energy band gap higher than 5 eV [7]. Furthermore, the different applications above mentioned require thin and uniform films with a low surface roughness [8]. Most techniques that involve a deposition from a chemical vapor lead in general to films with a low surface roughness and with excellent adherence on the substrates used [9]. The chemical decomposition of the reagents used to get the films then becomes very important, to predict their properties. Among the wide variety of these chemical techniques used to deposit thin films, the spray pyrolysis technique is considered a low cost and simple deposition technique that leads to thin films and coatings with good optical, structural, and electrical properties [10, 11].

Yttrium oxide (Y_2O_3), is considered an interesting material for different technological applications due to its unique properties such as a high melting point (2,410 °C) [12], wide energy band gap (5.5 eV) [13], high resistivity of 10^{11} – 10^{12} Ω -m, high dielectric strength, and high dielectric constant (up to 13) [9, 14]. Because of its transparency (in the ultraviolet and visible range of the electromagnetic spectrum), Y_2O_3 is a prospective material to be used as antireflection and protective layer [15]. In addition, recent studies consider Y_2O_3 , as a good candidate to replace SiO_2 in the microelectronic industry because of

G. Alarcón-Flores (✉) · M. Aguilar-Frutis ·
J. Guzmán-Mendoza
CICATA-IPN, Legaria 694 Colonia Irrigación, C.P. 11500
Mexico, D.F., Mexico
e-mail: alar_fbeto@yahoo.com

M. García-Hipólito · M. A. Canseco
IIM-UNAM, Apdo. Postal 70-360, Delegación Coyoacán,
C.P. 04150 Mexico, D.F., Mexico

C. Falcony
Departamento de Física, CINVESTAV, Apdo. Postal 14-470,
Delegación Gustavo A. Madero, C.P. 07000 Mexico, D.F.,
Mexico

its high dielectric constant [16]. Furthermore, Y_2O_3 has been studied as a host matrix to obtain high efficiency phosphors when doped with rare-earth elements [17].

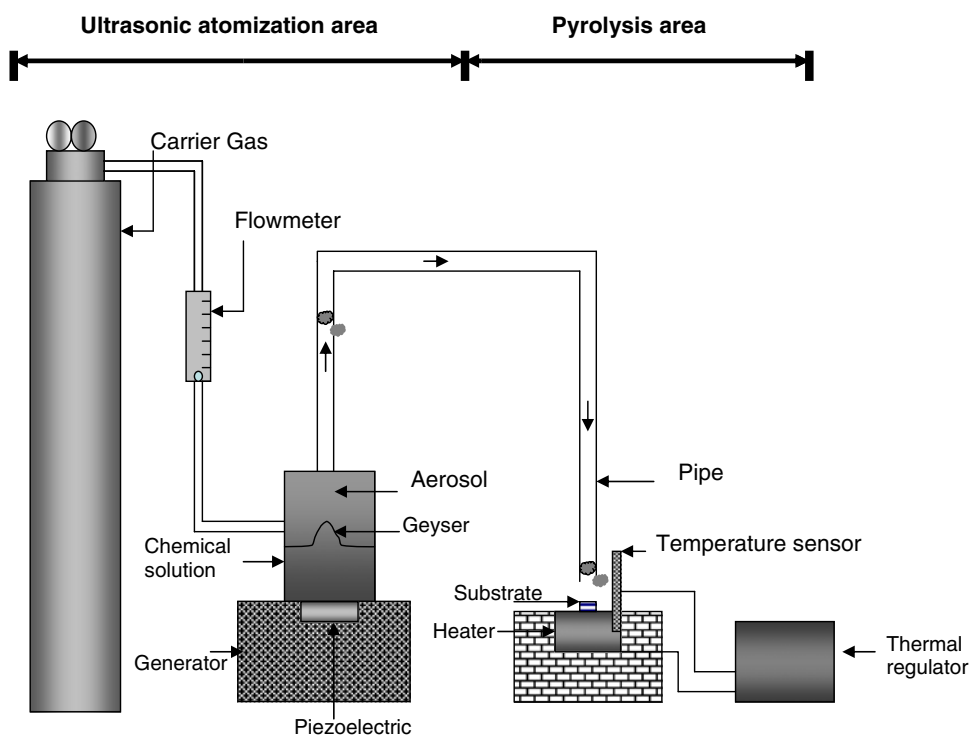
In this work, we report the synthesis of Y_2O_3 thin films by means of the ultrasonic spray pyrolysis technique from $Y(acac)_3$ as source of yttrium. For this task, the study of the thermal decomposition of the latter reagent was carried out first by means of thermogravimetry, differential scanning calorimetry, mass and infrared spectroscopies. The information obtained by these studies led us to determine the deposition conditions for Y_2O_3 thin films using the spray pyrolysis technique. Once the films were deposited they were physically characterized: the crystalline structure, the surface morphology, and some optical parameters were determined by X-ray diffraction, atomic force microscopy, infrared spectroscopy, and ellipsometry.

Experimental procedure

Hydrated yttrium acetylacetonate ($YC_{15}H_{21}O_6 \cdot XH_2O$), or $Y(acac)_3$, from Alfa Aesar, was used as source of yttrium. Five milligrams of this reagent was thermally decomposed in a TGA (Thermogravimetric Analysis) system (TA Instruments model 2950). Differential scanning calorimetry (TA Instruments model 2910), was also used. In both cases, a heating ramp rate of 10 °C/min was used for these thermal

analyses, which were carried out in an N_2 atmosphere. One gram of the yttrium salt was also analyzed by means of Mass Spectrometry (Jeol AX505HA spectrophotometer). In addition, infrared spectroscopy (Nicolet Magna IR) measurements were carried out in the $Y(acac)_3$ reagent. The Y_2O_3 thin films were deposited with a 0.03 M solution of $Y(acac)_3$ in *N-N* Dimethylformamide (NN-DMF). The deposition process was performed using the ultrasonic spray pyrolysis technique. In this technique a mist of the spraying solution is generated by means of ultrasonic vibrations. Figure 1 shows a diagram of the deposition set up. The mist is transported through a glass pipe to the heated substrates surface where a thin solid film is obtained by means of a pyrolytic reaction. A commercial ultrasonic humidifier (operated at 0.8 MHz) was used for this purpose. The substrates were c-Si(100) and (111) wafers. The substrates were previously cleaned before being loaded into the deposition chamber [18]. The deposition substrate temperature was 400, 450, 500, and 550 °C. Ultrapure air at 10 L/min was used as carrier gas. The index of refraction and thickness of the deposited films were measured by ellipsometry (Gaertner LSE stokes ellipsometer), at 632 nm. In general, the thickness of the Y_2O_3 films was around 1,000 Å. A Siemens D-5000 X-ray diffraction system was used for the determination of the crystalline structure. In addition, an Atomic Force Microscope (Veeco CP research), was used to obtain the characteristics of the films' surface morphology.

Fig. 1 Schematic diagram of the ultrasonic spray pyrolysis deposition process



Results and discussion

Figure 2 shows the thermogravimetric analysis of the $Y(acac)_3$ complex in an N_2 atmosphere. An initial transformation, occurring around 57 °C, involves a weight loss of about 10%, and it is probably due to loss of humidity or some volatile gas previously adsorbed by the yttrium salt. The next transformation occurs approximately at 92 °C with a weight loss of about 9%, attributed to the dehydration of the salt. The theoretical calculation of this weight loss is of 9.3%, which corresponds to $2H_2O$ molecules. Table 1 compares the experimental results and the corresponding theoretical analysis of the decomposition of the yttrium salt. A third weight loss, about 25% of the full weight of the yttrium salt, was observed around 240 °C. This loss corresponds, very probably, to the loss of one β -diketone molecule ($C_5H_7O_2$). In the high temperature range, from 340 °C to 590 °C, additional weight losses are observed. They are related mainly to the remaining complex ($Y(acac)_2$), that is being partially decomposed. The complete combustion of the metalorganic complex occurs about 600 °C, leaving a solid whose weight is about 25% of the original complex. This solid consists mainly of yttrium oxide (Y_2O_3) and some organic matter residues. A similar decomposition mechanism was observed previously in magnesium acetylacetonate, $Mg(acac)_2$ [19]. Figure 3 shows the differential scanning calorimetry (DSC) graph of the yttrium complex. In this figure an endothermic peak is observed at 89 °C. This peak seems to correspond to the weight loss due to humidity and/or an adsorbed gas. A second endothermic peak, at 99 °C, corresponds to the second weight loss shown by thermogravimetry and ascribed to dehydration. A third endothermic peak is observed at 126 °C corresponding probably to the melting point of the $Y(acac)_3$. The low melting point temperature of some β -diketones is an important property for being used during the synthesis of new products and for different applications [20]. Figure 4 shows the characteristic mass

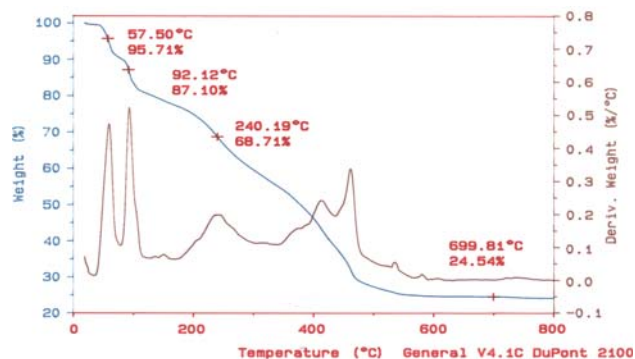


Fig. 2 Thermogravimetric analysis (TGA) of the yttrium acetylacetonate complex

Table 1 Thermogravimetric analysis of the yttrium acetylacetonate complex

Temperature (°C)	Measured weight loss (%)	Theoretical weight loss (%)	Interpretation
<60	~10	–	Humidity or adsorbed gas
~80–115	~9	9.3	Dehydration $2H_2O$
~240	~25	25.6	Loss of $C_5H_7O_2$
~340–590	~30	–	Degradation of $Y(C_5H_7O_2)_2$

spectrometry of the $Y(acac)_3$ salt. The positive peak ion observed at m/z 386 represents the molecular ion (M^+). After fragmentation, the most abundant masses are noted as follows: 371 (3.1%) (M^+-15), 287 (100%) (M^+-99), 187 (4%) (M^+-198), 100 (4.4%) (M^+-286), 85 (6.6%) ($M^+-286-15$), and 43 (7.8%) ($M^+-286-57$). As observed in Fig. 5, the $Y(acac)_3$ complex consists of three acetylacetonate ($acac$) molecules coordinated to one yttrium ion. The peak m/z at 287 corresponds exactly to two β -diketone ($C_5H_7O_2$) linked to one yttrium atom. This means that a complete β -diketone molecule was lost from the original complex, and it is related to the weight loss of 25% observed in the thermogram at about 240 °C. The remaining fragment, containing the yttrium atom, $Y(acac)_2$, is slowly degraded to form Y_2O_3 and organic residues. On the other hand the β -diketone lost seems to be split then into light fragments, for example the α ketone group ($C=O$) produces the fragment m/z 85, attributed to methyl loss from β -diketone, and to the fragment m/z 43 corresponding to the acylium group, which are all observed in the mass spectrum [21]. These results suggest that the $Y(C_5H_7O_2)_3$ is split in the $C_5H_7O_2$ fragment and in the $Y(C_5H_7O_2)_2$ complex. It is thought that this latter fragment is slowly decomposed leading finally to

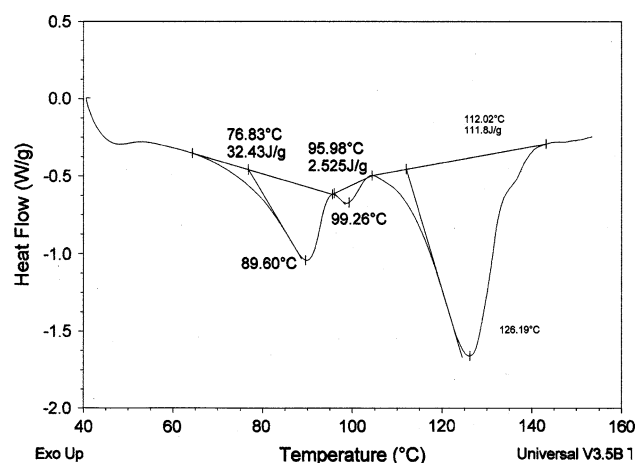


Fig. 3 Differential scanning calorimetry (DSC) of yttrium acetylacetonate

Fig. 4 Mass spectroscopy of yttrium acetylacetonate

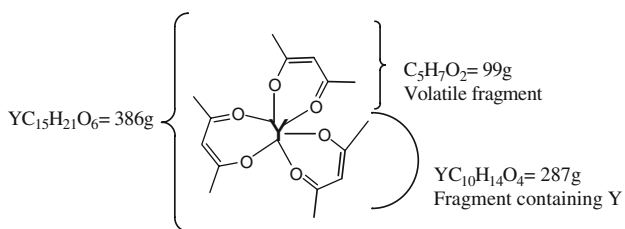
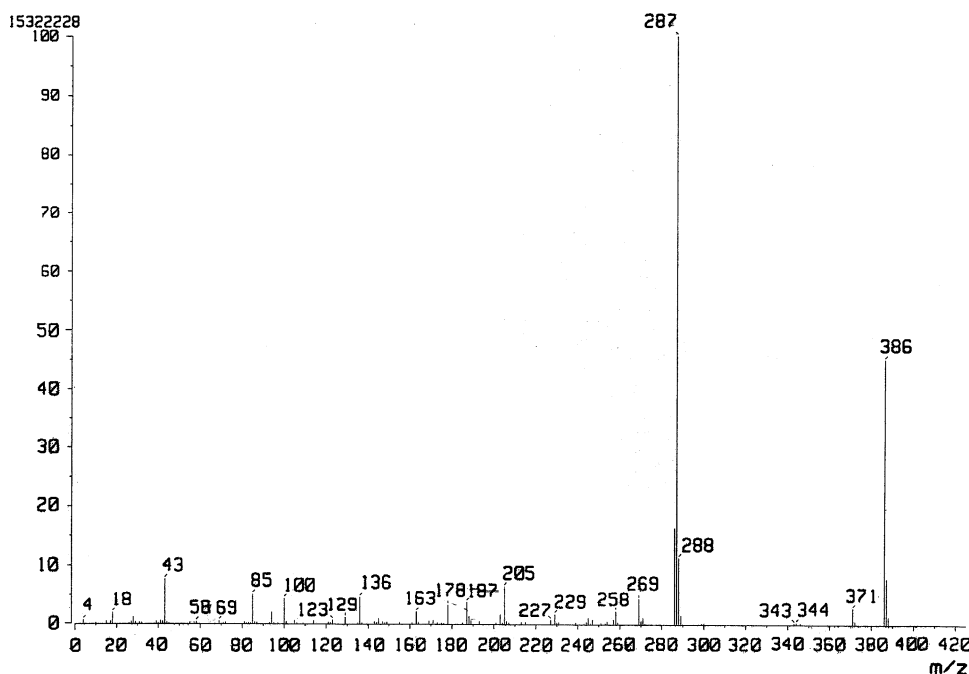


Fig. 5 Decomposition schema of the yttrium acetylacetonate structure

Y_2O_3 and organic residues. Figure 6 shows a series of infrared spectra, measured at room temperature, performed on the hydrated $Y(C_5H_7O_2)_3$ complex upon being heated at different temperatures, from room temperature up to 500 °C. The infrared bands are interpreted in Table 2 [22]. The bands in the spectrum are labeled with numbers 1 to 11 and 13. The spectrum (b), 155 °C, presents almost the same bands, as the ones observed in spectrum (a), 25 °C. This might be so because the complex was probably melted, but it did not decompose. On the other hand, the spectra labeled as (c), 240 and (d), 300 °C, show important transformations in its structure, probably because one β -diketone was lost. Several bands seen in (a) are no longer observed in (c) or (d), except for the bands that are due to ketone groups, but with reduced intensity. The spectrum (e), 500 °C, presents much higher transformations than the spectrum at 300 °C. However, the bands 3 to 5 continue appearing because they are related to $\nu(C=O)$, $\nu(C=C)$, and $\delta(CH_3)$ groups. However a new band, labeled as 12, and located around 560 cm^{-1} , is the one that is now present in the spectra. This band corresponds to the Y–O bonding from Y_2O_3 . These results show that the appearance of Y_2O_3 occurs close to 500 °C, but at the same time there

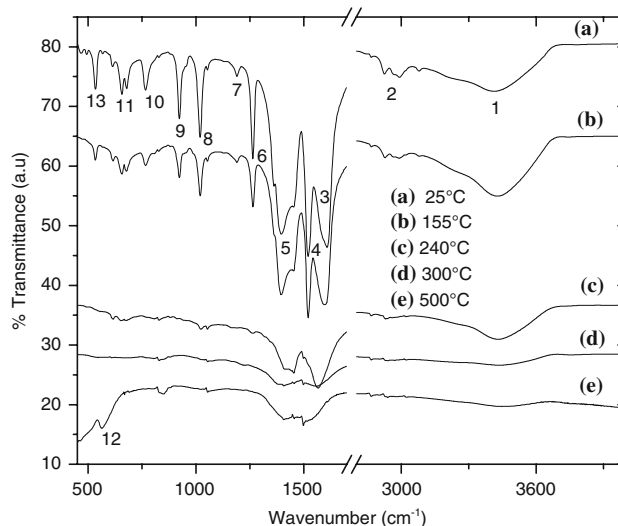
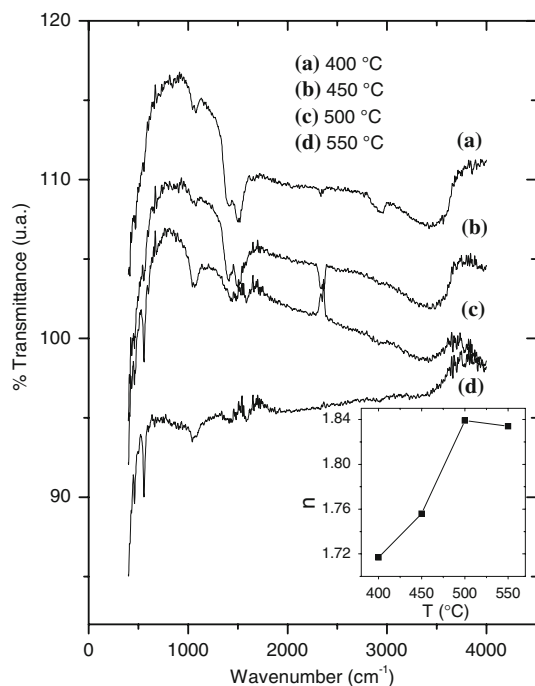


Fig. 6 Infrared spectra of yttrium acetylacetonate heated to different temperatures

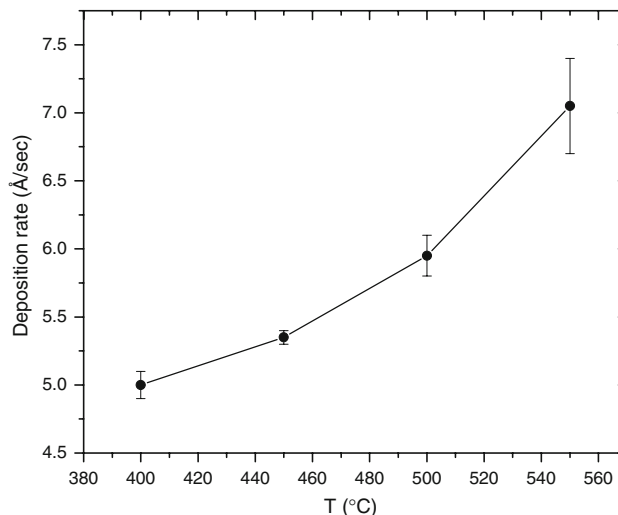
remains some organic matter due to the incomplete decomposition of the $Y(C_5H_7O_2)_3$ original complex. Figure 7 shows now the infrared spectra of the films deposited at different substrate temperatures. The IR spectra show two bands located approximately at 557 and 460 cm^{-1} . These bands, corresponding to the Y–O bonding, are more intense in films deposited at 500 and 550 °C, than when deposited at temperatures of 400 and 450 °C. This indicates that a larger number of Y–O bonds are synthesized in the films deposited at higher temperatures. These bands have already been reported for Y_2O_3 thin films obtained by other techniques, such as the sol–gel technique [23].

Table 2 Infrared spectroscopy analysis of the yttrium acetylacetonate complex

Band	Y(acac) ₃					Mode predominant
	25 °C cm ⁻¹	155 °C	240 °C	300 °C	500 °C	
1	~3,400	~3,400	~3,400	~3,400	~3,400	$\nu(\text{OH})$
2	~2,900	~2,900	–	–	–	$\nu(\text{CH}_3)$
3	~1,600	~1,600	~1,600	~1,600	~1,600	$\nu(\text{C}=\text{O}) + \nu(\text{C}=\text{C})$
4	~1,520	~1,520	~1,520	~1,520	~1,520	$\nu(\text{C}=\text{C}) + \nu(\text{C}=\text{O})$
5	~1,400	~1,400	~1,400	~1,400	~1,400	$\delta(\text{CH}_3)$
6	~1,260	~1,260	~1,260	–	–	$\nu(\text{C}-\text{CH}_3) + \nu(\text{C}=\text{C})$
7	~1,180	~1,180	–	–	–	$\delta(\text{CH}) + \nu(\text{C}-\text{CH}_3)$
8	~1,020	~1,020	~1,020	–	–	$\rho r\text{CH}_3$
9	~925	~925	–	–	–	$\nu(\text{C}=\text{C}) + \nu(\text{C}=\text{O})$
10	~770	~770	–	–	–	$\pi(\text{CH})$
11	~675	~675	~675	–	–	$\nu(\text{C}-\text{CH}_3) + \text{ring deformation} + \nu(\text{MO})$
12	–	–	–	–	~560	Y–O
13	~535	~535	–	–	–	$\nu(\text{MO}) + \nu(\text{C}-\text{CH}_3)$

**Fig. 7** Infrared spectra of yttrium oxide thin films deposited at different substrate temperatures. The inset shows the index of refraction of the films

In the spectra a broad band around $3,500\text{ cm}^{-1}$ is observed, characteristic of O–H groups. The presence O–H bonding in thin films, for example in SiO_2 , indicates the existence of some porosity in them [24]. In this case films deposited at 400 and 450 °C seem to be more porous than the films deposited at 500 or 550 °C. This is probably the reason why these films have lower indexes of refraction, which are shown in the inset of Fig. 7. The O–H groups

**Fig. 8** Deposition rate of yttrium oxide thin films as a function of the substrate temperature

have been reported by Niu et al., in the $3,100\text{--}3,600\text{ cm}^{-1}$ and $1,600\text{ cm}^{-1}$ regions for Y_2O_3 films. In this case the band centered at $3,460\text{ cm}^{-1}$ is due to vibration stretching (ν), and the one at $1,650\text{ cm}^{-1}$ is due to a bending mode (δ) [25]. Furthermore, the spectra in Fig. 7 show bands close to the $1,500\text{ cm}^{-1}$ region. These bands are characteristic of organic residues due to the raw materials used to synthesize the films [26]. For example, in Y_2O_3 films, bands located at $1,510$ or $1,410\text{ cm}^{-1}$ correspond to the asymmetric stretching vibrations of carbonyl CO (ν_{as}) [23]. The bands due to organic residues were reviewed by Guo et al., who found that they tend to decrease with the increase of the substrate temperature. It has been suggested that they are

due to an incomplete decomposition of metal β -diketonates which are used to obtain the films. According to the results presented above, the bands that were observed in the $1,500\text{ cm}^{-1}$ region in the infrared spectra correspond to the incomplete decomposition of the Yttrium acetylacetonate salt $[\text{Y}(\text{C}_5\text{H}_7\text{O}_2)_3]$ (Fig. 6). This confirms that organic residues are due to the yttrium reagent, and they still remain in the films. In addition, the spectra show that the content of organic residues drops when the substrate temperature to synthesize the Y_2O_3 film is increased. Figure 8 shows the deposition rate of the Y_2O_3 films as a function of the substrate temperature. Deposition rates lower than 10 \AA/s were determined from measurements of the final thickness of the films considering the deposition time. In addition, Fig. 9 shows a typical atomic force microscopy image of a film deposited at $500\text{ }^\circ\text{C}$. In general, the surface morphology of the films was very flat with a root squared surface roughness (rms) lower than 40 \AA . A low surface roughness is in general a stringent requirement for optical and microelectronic applications.

The X-ray diffraction patterns of the films are shown in Fig. 10. It can be observed that as the deposition temperature is increased, the crystalline structure of the films is improved. The peaks located at $2\theta = 29.1^\circ$, 48.5° , and 57.6° correspond to the (222), (440), and (622) reflections, respectively. These reflections correspond to the Y_2O_3 cubic phase, according to the JCPDS 43-1036 diffraction card (with a lattice parameter of 10.604 \AA). The cubic structure is also observed when Y_2O_3 is synthesized by means of other deposition techniques, such as r.f. magnetron sputtering [27] and laser ablation [28]. The grain size of the films, estimated from the Scherrer formula [29], was found in the range from 14 nm to 22 nm .

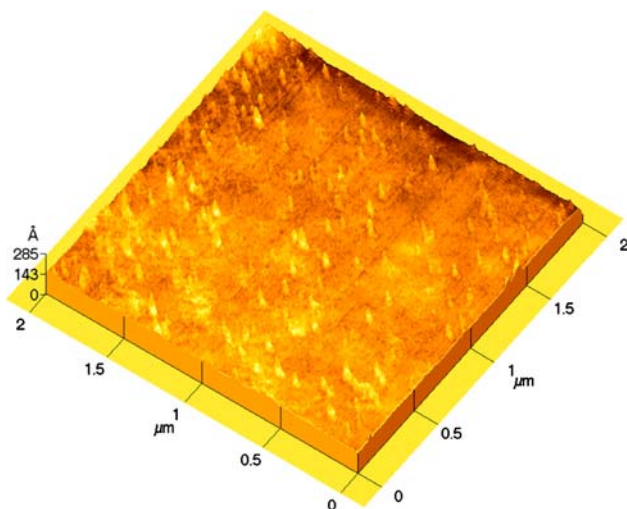


Fig. 9 Atomic force microscopy image of the surface morphology of yttrium oxide thin films deposited at $500\text{ }^\circ\text{C}$

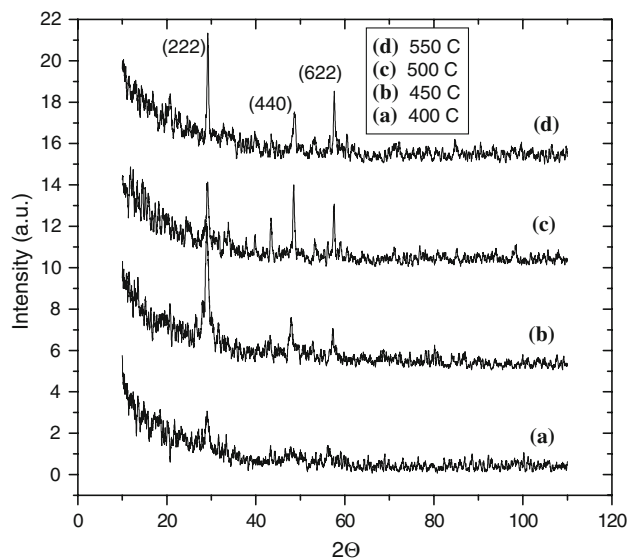


Fig. 10 X-ray diffraction patterns of yttrium oxide thin films deposited at different substrate temperatures

Conclusions

Thin films with good optical and structural characteristics were obtained with the spray pyrolysis technique from the decomposition of $\text{Y}(\text{acac})_3$. A detailed analysis of the thermal decomposition of $\text{Y}(\text{acac})_3$ indicates that it is first decomposed in a β -diketone and in $\text{Y}(\text{C}_5\text{H}_7\text{O}_2)_2$, leading, the latter complex, mainly to Y_2O_3 and carbon related residues at temperatures above $390\text{ }^\circ\text{C}$. The Y_2O_3 films were flat with a surface roughness lower than 40 \AA . The deposition rate was lower than 10 \AA/s , with a refraction index close to 1.8. The films obtained were polycrystalline mainly at temperatures higher than $450\text{ }^\circ\text{C}$, presenting the cubic phase of Y_2O_3 at high temperatures.

Acknowledgements The authors would like to thank warmly to CONACyT-México and to CGPI-IPN for the financial support through the scientific research projects (Grant Nos. 2005815, 20040278). The technical assistance of B. Esquivel, R. J. Fregoso, M. Guerrero, and A.B. Soto is also acknowledged.

References

- García-Hipólito M, Alvarez Fregoso O, Martínez E, Falcony C, Aguilar Frutis MA (2002) *Opt Mater* 20:113
- Duparre A, Welsch E, Walther HG, Kaiser N, Mueller H, Hacker E, Latuh H, Meyer J, Weissbrodt P (1994) *Thin Solid Film* 250:1
- Choi SC, Cho MH, Whang SW, Kang SB, Lee SI (1997) *Appl Phys Lett* 71:903
- Zhang S, Xiao R (1998) *J Appl Phys* 83:3842
- Ivanic R, Rehacek V, Novotny I, Breternitz V, Spiess L, Knedlik CH, Tvarozek V (2001) *Vacuum* 6:229
- Lou L, Zhang W, Brioude A, Le Luyer C, Mugnier J (2001) *Opt Mater* 18:331
- Robertson J (2006) *Rep Prog Phys* 69:334

8. Aguilar-Frutis M, García M, Falcony C (1998) *Appl Phys Lett* 72(14):1700
9. Alarcón-Flores G, Aguilar-Frutis M, Falcony C, García Hipólito M, Araiza JJ, Herrera-Suárez YHJ (2006) *J Vac Sci Technol B* 24(4):1875
10. Blandenet G, Court M, Lagarde Y (1981) *Thin Solid Film* 77:81
11. Wang S-Y, Lu Z-H (2002) *Mater Chem Phys* 78:542
12. Gurvitch M, Manchanda L, Gibson JM (1987) *Appl Phys Lett* 51(12):919
13. Swamy V, Dubrovinskaya NA, Dubrovinsky LS (1999) *J Mater Res* 14(2):456
14. Araiza JJ, Aguilar-Frutis MA, Falcony C (2001) *J Vac Sci Technol B* 19(6):2206
15. Ivanic R, Rehacek V, Novotny I, Breternitz V, Spiess L, Knedlik CH, Tvarozek V (2001) *Vacuum* 6:229
16. Gaboriaud RJ, Paumier F, Paillaoux F, Guerin P (2004) *Mater Sci Eng B* 109:34
17. Hao J, Studenikin SA, Cocivera M (2001) *J Lumin* 93:313
18. Fountain GG, Rudder RA, Hattangady SV, Markunas RJ (1988) *J Appl Phys* 63:4744
19. Stryckmans O, Segato T, Duvigneaud PH (1996) *Thin Solid Films* 283(1):7
20. Mehrotra RC, Bohra R, Gaur DP (1978) *Metal β diketones and allied derivatives*. Academic Press Inc., London, p 58
21. McLafferty F, Turecer F (1993) *Interpretation of mass spectra*. University Science Books, USA, p 52
22. Nakamoto K (1986) *Infrared and Raman spectra of inorganic and coordination compounds*. John Wiley and Sons, USA, p 259
23. Guo H, Zhang W, Lou L, Brioude A, Mugnier J (2004) *Thin Solid Films* 458:274
24. Adams AC (1983) *Solid State Technol* 26:135
25. Niu D, Ashcraft RW, Parsons GN (2002) *Appl Phys Lett* 80(19):3575
26. Durand C, Dubourdieu C, Vallee C, Loup V, Bonvalot M, Joubert O, Roussel H, Renault O (2004) *J Appl Phys* 96(3):1719
27. Hornig RH, Wu DS, Yu JW, Kung CY (1996) *Thin Solid Films* 289:234
28. Araiza JJ, Cardenas M, Falcony C, Mendez Garcia VM, Lopez M, Contreras-Puente G (1998) *J Vac Sci Technol A* 16:3305
29. Cullity BD (1954) *Elements of X-ray diffraction*. Addison-Wesley, Publishing Company Inc., p 261